

## Retraction

# Retracted: Secure Data Deduplication System with Cyber Security Multikey Management in Cloud Storage

### Security and Communication Networks

Received 10 October 2023; Accepted 10 October 2023; Published 11 October 2023

Copyright © 2023 Security and Communication Networks. This is an open access article distributed under the Creative Commons Attribution License, which permits unrestricted use, distribution, and reproduction in any medium, provided the original work is properly cited.

This article has been retracted by Hindawi following an investigation undertaken by the publisher [1]. This investigation has uncovered evidence of one or more of the following indicators of systematic manipulation of the publication process:

- (1) Discrepancies in scope
- (2) Discrepancies in the description of the research reported
- (3) Discrepancies between the availability of data and the research described
- (4) Inappropriate citations
- (5) Incoherent, meaningless and/or irrelevant content included in the article
- (6) Peer-review manipulation

The presence of these indicators undermines our confidence in the integrity of the article's content and we cannot, therefore, vouch for its reliability. Please note that this notice is intended solely to alert readers that the content of this article is unreliable. We have not investigated whether authors were aware of or involved in the systematic manipulation of the publication process.

Wiley and Hindawi regrets that the usual quality checks did not identify these issues before publication and have since put additional measures in place to safeguard research integrity.

We wish to credit our own Research Integrity and Research Publishing teams and anonymous and named external researchers and research integrity experts for contributing to this investigation.

The corresponding author, as the representative of all authors, has been given the opportunity to register their agreement or disagreement to this retraction. We have kept a record of any response received.

### References

- [1] R. N. Kumar, T. Sathiya, H. C. Mohanta et al., "Secure Data Deduplication System with Cyber Security Multikey Management in Cloud Storage," *Security and Communication Networks*, vol. 2022, Article ID 9790398, 11 pages, 2022.

## Research Article

# Secure Data Deduplication System with Cyber Security Multikey Management in Cloud Storage

R. Nandha Kumar,<sup>1</sup> T. Sathiya,<sup>2</sup> Harish Chandra Mohanta ,<sup>3</sup> Sayed Sayeed Ahmad ,<sup>4</sup> Ankit Kumar ,<sup>5</sup> Ghalib H. Alshammri ,<sup>6</sup> and Henry Kwame Atiglah <sup>7</sup>

<sup>1</sup>Department of Computer Science and Applications, Vivekanandha College of Arts and Sciences for Women (Autonomous), Tiruchengode, Tamil Nadu, India

<sup>2</sup>Department of CSE, Sona College of Technology, Salem, Tamil Nadu, India

<sup>3</sup>Department of Electronics and Communication Engineering, Centurion University of Technology and Management, Gajapati, Odisha, India

<sup>4</sup>College of Engineering and Computing, Al Ghurair University, Dubai, UAE

<sup>5</sup>Department of Computer Engineering and Applications, GLA University Mathura, Mathura 281406, Uttar Pradesh, India

<sup>6</sup>Department of Computer Science, Community College, King Saud University, Riyadh 11437, Saudi Arabia

<sup>7</sup>Department of Electrical & Electronics Engineering, Tamale Technical University, Tamale, Ghana

Correspondence should be addressed to Henry Kwame Atiglah; [hkatiglah@tatu.edu.gh](mailto:hkatiglah@tatu.edu.gh)

Received 17 April 2022; Revised 29 June 2022; Accepted 5 July 2022; Published 12 August 2022

Academic Editor: Mukesh Soni

Copyright © 2022 R. Nandha Kumar et al. This is an open access article distributed under the Creative Commons Attribution License, which permits unrestricted use, distribution, and reproduction in any medium, provided the original work is properly cited.

Object detection is essential in a video surveillance system. To recognize an item in a movie, we first examine each picture pixel by pixel. The Secure Data Deduplication system in segmentation is the process of separating distinct picture components into pixels in digital image processing. The performance of segmentation is influenced by irregular and/or poor lighting. These characteristics have a significant impact on the video surveillance system's real-time object detection process. A multikey management system based on a modified ResNet model is presented in this research (M-ResNet). Cyber security is a suggested algorithm application that is used to improve images that are influenced by a lack of light. The experimental findings reveal a significant improvement in detecting objects in the video stream as compared to the present technique output and modification architecture of the ResNet model. The suggested model achieves superior results in measures like precision, recall, and pixel accuracy, as well as a decent increase in object recognition.

## 1. Introduction

Indexing of fingerprints identifies duplicate and nonduplicate data chunks after the chunking and fingerprinting steps of the deduplication system. An earlier deduplication technique stores the complete chunk fingerprint index in memory for quick redundant data identification. However, due to the exponentially expanding index size of the deduplication system, fast increasing data volume results in a high number of fingerprints created, which overflows the RAM capacity. As a result, frequent access to low-speed storage drives for fingerprint-index search drastically limits throughput. Some data deduplication systems have limited accessing throughput to the on-disk fingerprint index,

resulting in a significant performance bottleneck. Random accesses to the on-disk index are substantially slower than those to the on-RAM index. However, the additional hardware costs associated with on-RAM indexing have grown too high. The texture of the fingerprint image is stored on the hard disc of the system, which improves the training and testing process. On the other hand, on-disk fingerprint indexing lowers RAM overhead costs for deduplication indexing. Flash-based indexing strategies raise the hardware expenses of deduplication systems. Cluster deduplication technologies provide scalability for vast storage systems at the expense of a low deduplication ratio or need more resources to achieve a high deduplication ratio. To improve storage space efficiency, deduplication technology is mostly used

on disk-based secondary permanent storage. However, typical on-disk indexing techniques are plagued by two significant issues. The duplicate-lookup disc bottleneck is the first technical difficulty, and the storage node island effect is the second important concern. Traditional indexing methods save the complete index of data pieces.

As a result, as data volume grows, the index becomes too huge to contain whole hash values. In this circumstance, the deduplicate process finds it difficult to handle the search fingerprints in an on-disk index, reducing efficiency and lowering system performance. The second problem is overcoming the storage node island effect in order to reduce duplicates inside main or backup storage, which is not possible in distributed multiple storage nodes.

Image processing in low-light environments is a difficult problem, especially in video surveillance systems. Because of the absence of light, the picture quality is automatically reduced. A large amount of picture information has been warped, affecting image processing applications such as object recognition, object tracking, and segmentation. Because of the automated identification of anomalous occurrences, object detection plays a significant role in video surveillance systems. Detecting objects in a video stream requires additional calculations because of the vast quantity of data, and the picture captured from the video sequence must be of excellent quality. The illumination in a real-world situation is inconsistent, especially at night. Even if the video camera quality is excellent, the retrieved pictures from the video stream may be of poor quality. Image segmentation is the most important phase in image data processing [1]. The fundamental aim of image segmentation is to divide the picture into various semantic sections. Low-quality photos, especially those collected from recorded movies at night, will have an impact on the accuracy of image interpretation. Various ways may be employed to improve visualization. For recognizing lighting sections in segmented scenes, the nonuniform illumination previous model [2] is presented. Convolutional neural networks are a mathematical model that consists of a large number of processing units that operate simultaneously on various sets of data [3]. CNN has a number of layers that recognize essential aspects of picture data without the need for human intervention [4]. The greater the number of layers, the greater the accuracy of the result. When deeper networks are added, performance rises to a certain point before dramatically degrading [5]. In other words, adding additional layers results in more training errors.

According to Figure 1, the 56-layer CNN architecture has a higher error rate on both testing and training datasets than the 20-layer CNN architecture. ResNet (residual network) is a kind of deep learning model [6] composed of residual blocks. There is a direct link that bypasses certain model levels. The residual block is a collection of layers in which the layer's output is combined with another layer in the block [7]. This bypass connection is known as a skip connection or shortcut connection, as seen in Figure 2. These residual blocks, when joined, produced residual networks.

The training phase of a residual network is less difficult than that of regular deeper neural networks, and adding

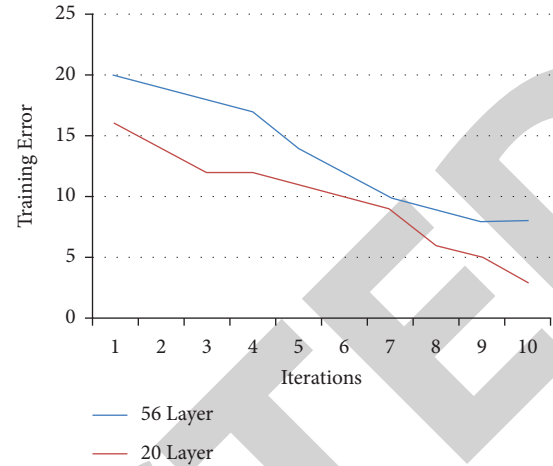


FIGURE 1: Training error in 56- and 20-layer deeper network.

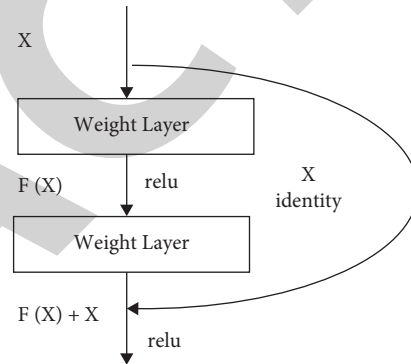


FIGURE 2: Basic building block of residual learning.

additional layers leads to higher training errors. Residual networks (ResNets) are used to mitigate training mistakes in deeper networks. ResNet is an efficient method for finding features in the salient region [8]. To increase the high-level and low-level semantic characteristics, two distinct residual networks are applied. ResNet offers shortcut connections that allow it to circumvent the insufficient training layers by mapping high-level features to low-level features. We need to improve the picture from low quality owing to limited light to optimum quality so that it can be processed effectively to identify the items. Several image-enhancing techniques have previously been developed, which may be divided into two categories: statistical-based approaches and decomposition-based approaches [9]. The lighting component is detected, and noise is minimized using volume-based subspace analysis.

This paper's significant contributions are summarised as follows: We offer modified ResNet (M-ResNet), which includes bilateral and adaptive supersampling procedures as additional convolution layers inside the original ResNet CNN architecture.

The proposed operation consists of residual units that improve image quality from low illumination to normal illumination. If the image already has a good lighting environment, the proposed residual units are skipped to avoid unnecessary computations. The introduced residual unit

removes noise and strengthens the edges of each object present in the captured image. While comparing current approaches, the suggested method achieves the desirable improvements.

The Content Defined Chunking (CDC) algorithm divides a data stream into variable-size chunks addresses and the Fixed-Size Chunking (FSC) boundary-shifting issue by stating deduplication efficiency of storage systems is greatly improved by using chunk boundaries. To deliver the essential services, a good CDC algorithm should have the main qualities and the following characteristics for effective data deduplication:

- (1) Defined content: the CDC algorithm should create chunk boundaries depending on data, which are contents to eliminate the boundary-shift issue.
- (2) Reduced calculation overhead: current CDC algorithms verify almost every byte of data. The input data stream to determine the chunk boundary rapidly rises. Due to the long execution time, deduplication throughput is limited. Throughput is increased using the chunking algorithm with the reduction in time consumption.
- (3) Variation in chunk size: variation in chunk size has a significant influence on identifying maximal redundancy and boosting deduplication system speed by increasing deduplication efficiency, i.e., TTTD.
- (4) Effective for low-entropy strings: the data stream's contents may change from time to time, consisting of low-entropy strings with a significant number of repeating bytes. It is preferable to discover and delete these duplicate strings to attain greater results.
- (5) Efficiency of deduplication.
- (6) Fewer chunk size restrictions: maximum and minimum criteria are often used, enforced to decrease computing costs by avoiding too tiny parts.

By avoiding too big data, you can improve your deduplication ratio. These thresholds, on the one hand, restrict lessen the variation in chunk size but on the other hand makes the chunk borders position dependent. As a result of not being completely content specified, this affects deduplication efficiency.

The remainder of the paper is organized as follows: Section 2 discusses the object identification process using several approaches such as low light, Gaussian distribution, probabilistic model, background removal, and graph-based algorithms. Section 3 outlines the suggested work; it demonstrates how the picture may be improved from low light by superimposing large- and small-scale bilateral operation components. Section 4 validates the proposed model using various kinds of datasets and compares it to related data. Section 5 summarizes the paper's actual work and suggests potential future possibilities.

## 2. Related Work

*2.1. Object Detection in Low-Light Environment.* Detecting things in low-light conditions is a difficult problem in a surveillance system. Due to inadequate lighting, the acquired photographs include a lot of black patches and noise in the picture information. Existing deep learning approaches are incapable of performing effectively in low-light environments. The inconsistent distribution of brightness makes object categorization challenging in this setting. The collected picture from a low-light environment must be improved in order to recognize objects accurately. The following drawbacks exist in the process of upgrading low-light photos using deep learning methods:

- (i) Complex structure and a large number of parameters are required
- (ii) More layers and computing are required
- (iii) The training requires a paired dataset, which is challenging to achieve in reality

The aforementioned difficulties cause object detection systems to perform poorly and waste more computer resources. As a result, a simple technique is required to address these difficulties. The volume-based subspace [9, 10] solves the first and second concerns by segregating the light area and noise in the picture. The light component in the subspace may be detected and separated using principle energy analysis [11]. In the volume-based subspace, noise may be reduced by using an adaptive truncation approach [12]. Deep noise suppression [13] and regularized lighting optimization [14] are two methods for noise reduction. To improve the picture in a low-light situation, a combination of refined lighting and an improved reflection map may be used. A Night Vision Detector (NVD) based on RFB-Net [15, 16] employs both the context fusion and feature pyramid networks. Various lighting data may be modelled individually in this case, even if they interfere with each other throughout the training phase. The third problem may be addressed by the new RetinexGAN and EnlightenGAN models [17]. The training phase employs completely unpaired datasets, and the model employs a basic generative adversarial network. Another technique, built by a pipelined convolutional neural network with a Gaussian kernel and based on multiscale Retinex and discrete wavelet transformation [18], conducts denoising and picture enhancing nets. The image enhancement function in this architecture is learned from a pair of dark and bright images.

*2.2. Detection of Objects by Applying the Gaussian Distribution.* Changes in lighting and noise corruption have a significant impact on the effectiveness of the change detection algorithms. The current noise has a significant impact on the interaction between neighboring pixels. The saliency augmentation method [19, 20] improves object saliency weight information. By suppressing background information using a Gaussian mixture model [21], the feature difference between modified and unaffected areas may be identified. Denoising methodologies [22] such as blind global image fusion [23] and Fusion Net gives better

results. It uses a Bayesian method to assess the optimality of the training network's noise level and unobserved Gaussian noise levels. When compared to the Point Distribution Model, the Gaussian Process Morphable Model (GPMM) [24] effectively specifies the covariance function. In modern registration systems, this GPMM incorporates several kernel functions. Shape variations may be accurately simulated using the Gaussian process. The multivariate Gaussian technique [25] may describe normal data in deep feature representations. It is also efficient to transfer learned representations from big datasets like ImageNet to small datasets. The present Gaussian mixture modeling (GMM) approach for background removal is heavily influenced by noise and dynamic background [26]. GMM background subtraction method demonstrates the background reduction by eliminating zeros in the pixels value [27]. For successful results, the background model is first rebuilt by averaging picture blocks, then the noise information is removed, and lastly, the background information is updated.

### 2.3. Detection of Objects Using Probabilistic Methods.

Because medical pictures include dynamic image intensity and changing boundary information, standard image segmentation algorithms are unsuitable for Ultra Sound images. To address this problem, Bayesian CNN [28] may be used on Ultra Sound pictures to produce random predictions based on probability distributions. The likelihood may be calculated using a combination of MRI volumes and femoral cartilage outlines in this method. The maximization (EM) approach is often used to simulate brain image expectation. For whatever amount of noise, these approaches also need certain unique denoising algorithms [29]. Another technique [30] is to supplement the probabilistic atlas, which has information about healthy tissue, with a latent atlas, which contains information about lesions. The semantic meaning of the tissues is provided by this generative probabilistic model and discriminative extensions. The author [31] creates a novel method that uses the probability distribution of both the object and the backdrop to get a more accurate segmentation result. The suggested approach maximizes the difference between the background and Gaussian mixture distributions. This probability-based approach is used on several imaging modalities such as dermoscopy, chromoendoscope, and MRI. The presence of thin clouds in remote sensing image processing might reduce the efficacy of cloud identification methods. Before processing remote sensing photos, the cloud material must be removed. The author [29] offers a deep learning cloud detection technique that combines an attention mechanism with probability upsampling. The method is concerned with the link between spatial dimension and multispectral picture of spectral segments. The full convolutional network converts single label retrieval into multilabel retrieval [32], and selecting the proper sample pattern is critical for reconstructing high-quality pictures [33]. A sampling strategy based on a probability mass function may dynamically modify the sample rate depending on data acquired in advance. This static incremental sampling approach with probability mass

function eliminates sampling latency, allowing for high-quality picture reconstruction.

### 2.4. Detecting Objects Using Background Subtraction Methods.

The background subtraction approach is crucial for distinguishing between a static backdrop and a moving item. Background modifications will make this procedure more complicated and generate erroneous findings. As a result, the dynamic Auto Regressive Moving Average (ARMA) [34] model is used, which uses the spatial and temporal correlation of input pictures to create an appropriate model for the background image. The adaptive least mean square technique may be used to update the dynamic properties of the backdrop. The fuzzy histogram describes the temporal properties of the pixels by using fuzzy C means clustering with fuzzy nearness degree (FCFN) [35] background removal technique. It addresses the categorization problems for background and foreground items. Because of the enormous number of bands in hyperspectral images (HSIs), the dimension must be reduced before processing. After reducing the dimensionality of the HSI, the hyperspectral visual attention model (HVAM) [36] is used in anomaly detection to highlight the prominent features. We remove the noise using a curvature filter, and the first result may be achieved with the background subtraction approach. To reach the final result, the given partial result may be submitted to the adaptive weight approach. Lighting changes, both fast and gradual, have an effect on the background subtraction models. The adaptive local median texture feature [31] approach is presented to address this problem. The adaptive parameter threshold for foreground pixels is extracted. Using ALMT characteristics in foreground pixels, the background model samples are compared to video picture sequences. To get the optimum object identification performance in low-light conditions, the appropriate background removal algorithms and parameters must be used. The author [37] investigated several background subtraction algorithm settings in order to develop an optimum background subtraction technique with the essential characteristics for detecting falls at night.

### 2.5. Graph-Based Network Object Detection.

Because the input flow between various neurons in a convolutional neural network may be viewed as a graph, building graph-based convolutional neural networks (GCNNs) is an emerging approach in image processing. GCNN may be separated into two categories depending on the filters used: spatial-based techniques and spectral-based approaches. The spatial technique is based on the aggregate of neighboring pixels. However, the spectral-based technique operates on an undirected graph. The lack of direction in the graphs has a significant impact on the learning process. The directed graph convolution network is powered by a fast localized convolution operator that can grow to huge graph sizes. There may be information loss of object boundaries in video salient object detection models. The author [38] combines the benefits of graph models with deep neural networks. The suggested solution incorporates a unified multistream

architecture for video SOD. This design operates inside the context of GCN, which provides a technique for efficiently grouping the common superpixels. The study in [39] introduces a new attention module for encoding superpixels. Finally, smoothness awareness regularization ensures the homogeneity of the main items. Skeleton-based action recognition systems often use hierarchical GCN, which may result in joint feature information loss after lengthy diffusion. To increase the local context information of joints, the author [40] offers multiscale mixed dense graph CNN. Two modules, spatial and attention, are used to fine-tune the spatial-temporal aspects. This suggested approach offers a changeable kernel size for each layer, resulting in a flexible temporal graph [22].

Few changes are required to improve image processing efficiency for image denoising challenges. To accomplish the network's strong learning capacity, graph convolution layers may be implemented in trainable neural network design [39, 41–43], which discovers the relationship between hidden characteristics of the network. Every pixel is represented as a vertex in a graph convolution network [41], and dynamically determined similarities are represented as edges. The advantages of incorporating graph convolution into an existing CNN include dynamic generation of neighborhood graphs, the creation of nonlocal filters that aggregate feature weights [39], and the avoidance of preset parameter operations. The architecture employs both local and nonlocal similarities for adaptable functioning [42]. We combine the benefits of GNN and CNN [43] to address knowledge base completion using out-of-knowledge-based entities [44]. To transfer knowledge to entities that do not have knowledge, a novel technique is given that uses a weight matrix to describe the relationships in the KBC model. After learning the information between nodes in this design, transition matrices are used to build more expressive embeddings. The proposed transition-based knowledge graph model solves the knowledge base completion tasks by employing these parameter values [45].

### 3. Proposed Work

This proposed work uses an optimization strategy to offer efficient data deduplication. For rapid convergence, an evolutionary DE technique is applied. It is stable, is simple to use, and lends itself nicely to parallel processing, making it ideal for Hadoop technology in cloud computing. The deduplication system receives the input data. The whole procedure is broken into the following steps.

**3.1. Effective Chunking.** Using two thresholds and two divisors with appropriate values, the input data stream is split into variable size pieces. The differential evolution algorithm searches for these parameters.

The values of divisor and threshold are taken as optimum values using differential evolution.

**3.2. SHA-1 Secure Hash Value Creation.** In secure cryptographic hash functions, each chunk's hash value is computed using SHA-1.

In certain circumstances, MD5 produces the same hash value for various chunks, which causes confusion and degrades speed. SHA-1 is used to generate safe, collision-free hashes of data chunks. A duplicate chunk is identified by locating its fingerprint in the key-value storage.

**3.3. Redundancy Identification and Removal with Bucket Indexing.** Based on bucket indexing, generated hash values are stored in the correct bucket from bucket 0 to bucket 9 and bucket A to bucket F by measuring the leftmost digit of the hash value, i.e., 9aca34...ef, 4ade923...cf, b23a3ce...cd1 hash value in bucket 9, bucket 4, bucket B. Duplicate hash values must be recognised and deleted using the Map and Reduce function. The driver provides Map and Reduce jobs to the relevant Data Nodes in the cluster during a MapReduce process.

**3.4. ResNet Architecture.** We can perform complicated problems in image processing activities such as categorization and identification of specific objects by adding additional layers to deep learning architecture. However, adding additional layers to the neural network causes accuracy loss and a difficult training period [46]. The ResNet architecture's residual blocks solve this problem. The ResNet architecture consists of 34 layers with quick connections between them. These short-cut connections are referred to as residual blocks. Figure 3 depicts an overview of the ResNet architecture [47].

Object identification accuracy increased by improving lighting effects and avoiding noise in the image [23]. Bilateral, adaptive, supersampling, and symmetric local binary patterns are novel layer operations, as depicted in Figure 4. Bilateral filtering creates a noise-reducing smoothing process while preserving edges. As a result, the skeleton of the items seen in the video frames may be preserved and the objects can be precisely recognized.

### 3.5. Proposed Architecture

**3.5.1. Bilateral Filtering.** The input picture from the video series is treated to a nonlinear bilateral filtering technique. This procedure increases smoothness while retaining edge information. The average of the neighboring pixels is computed in this method, which may be substituted by the original pixel. As a result, this bilateral procedure is also known as the weighted average of pixels [48].

$$\% \quad (1)$$

Two neighborhood pixels are taken and compared to get similar feature values during processing [49]. The bilateral filter operation is given by

$$BF[I_{\text{input}}]_p = \frac{1}{w_p} \sum_{x_i \in \Omega} I(x_i) F_r(\|I(x_i) - I(x)\|) g_s(\|x_i - x\|), \quad (2)$$

$$W_p = \sum_{x_i \in \Omega} F_r(\|I(x_i) - I(x)\|) g_s(\|x_i - x\|). \quad (3)$$

As illustrated in Figure 5, the input picture may be divided into two layers: a smoothed version called the

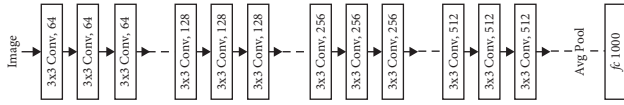


FIGURE 3: 34-layer residual network.

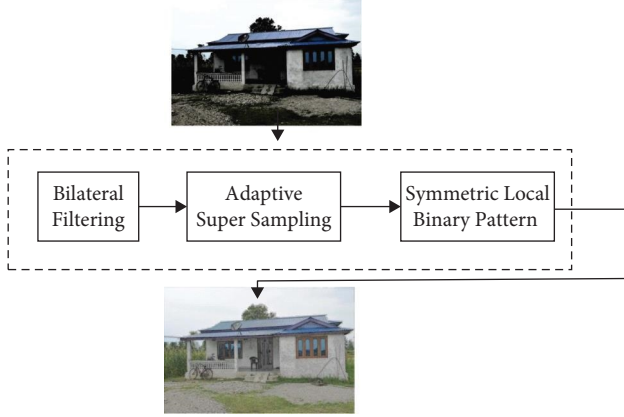


FIGURE 4: Additional layer operation.

large-scale component and a residual version called the small-scale component [50]. These remaining bits include noise and show the structure of the input picture, which is useful throughout the denoising process. Bilateral filtering combines a domain filter with a range filter. It computes and replaces the mean of comparable and neighboring pixel values for a given pixel. To apply the suggested work to a video surveillance system, sample photos are acquired ahead of time under optimal lighting conditions [51]. During surveillance, especially at night, the suggested system analyses the picture at a certain time interval using the current and sample image frames. The small size component of the sample picture may be overlaid on the big scale component of the current image frame to provide an upgraded image that precisely incorporates all of the item information, allowing the object identification procedure to be carried out. The full procedure is shown in Figure 6.

**3.6. Adaptive Super Sampling.** The result of bilateral operation may lead to pixelated edges, which causes aliasing of visual data. Aliasing happens as a result of continuous smooth curves and lines. A few samples are obtained for each pixel; if the samples have similar characteristics, the output pixel value is determined; if the samples are different, additional samples are needed to find the target pixel value [52]. As a result, it is not required to collect additional samples at all times. As a result, adaptive supersampling gives the pixel margin and preserves the object edges. The average of a function evaluated at a collection of points  $x_1, \dots, x_N$  is used to estimate the integral of a function  $f$ . Figure 7 shows the output of adaptive supersampling.

This can be calculated by aggregating the image function  $p(x, y)$ , that can represent the radiance of the particular

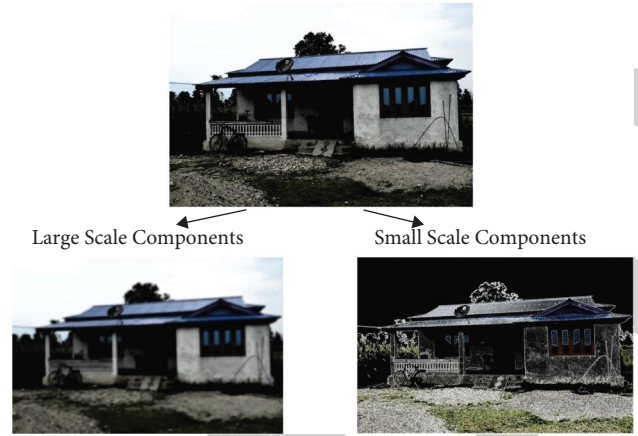


FIGURE 5: Output of the bilateral filter.

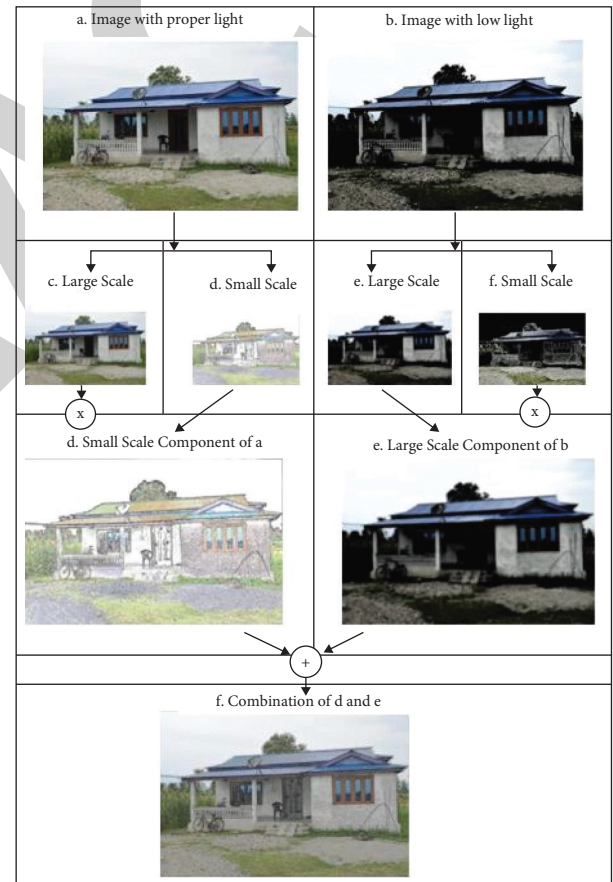


FIGURE 6: Modified image generation.

point  $(x, y)$  in the image pixels. The radiance  $L$  can be calculated by

$$L = \int_A p(x, y) f(x, y) dx dy. \quad (4)$$

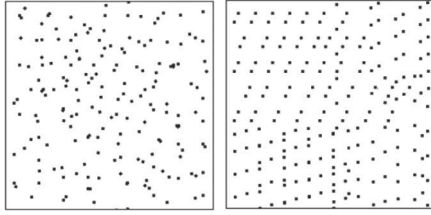


FIGURE 7: Output of adaptive supersampling.

Here,  $f(x, y)$  is an antialiasing filter and  $A$  is a supporting area of the filter. The random samples based on the Monte Carlo method [9],  $X_i, i = 1, \dots, n$ , obtains

$$L = \frac{1}{n} \sum_i X_i. \quad (5)$$

The samples are disseminated to corresponding kernel filters.

**3.6.1. Symmetric Local Binary Pattern.** It labels the pixels of an image by thresholding the neighborhood of each pixel and considers the result as a binary number [53]. The LBP operator in a video surveillance application can find the variations during illumination changes.

LPB can be calculated by identifying the difference between the intensities of pixels of neighborhood pixels. Let  $I_0$  represent the intensity of a particular pixel, and the neighbors are represented as  $i_n$ , where  $n$  represents the position of the neighbor. Figure 8 represents the size of  $n$  as 8. If the neighboring pixel value is equal or greater, the value is set to one, or otherwise, it is zero. Figure 9 represents the matrix allocation of pixel values.

$$LBP = \sum_{i=0}^{p-1} s(n_i - G_c) 2^i, \quad (6)$$

$$s(x) = \begin{cases} 1, & \text{if } x > 0, \\ 0, & \text{otherwise.} \end{cases}$$

**3.6.2. Experiment and Results.** To demonstrate the difference between the existing ResNet architecture and the modified ResNet (M-ResNet) architecture when processing low illumination images in a video surveillance system, we selected more images from the three different datasets coco, CIFAR, and WildTrack for testing to see if there were any effective improvements after the ResNet architecture was modified [54]. The outcomes of the tests are compared to the current methodologies. The coco dataset contains 5000 photos that are utilized throughout the training phase. Figure 10 shows how three distinct photos with poor lighting may be applied to current and customized ResNet architectures. Figure 10 shows two variants of the same picture selected from the coco dataset for experimentation [55]. The input image is preprocessed here using the usual lighting condition (Figure 10(a)). This picture has appropriate illumination and three zebras are detected, with the probabilities of the three items stated as 99.9, 99.8, and 99.4

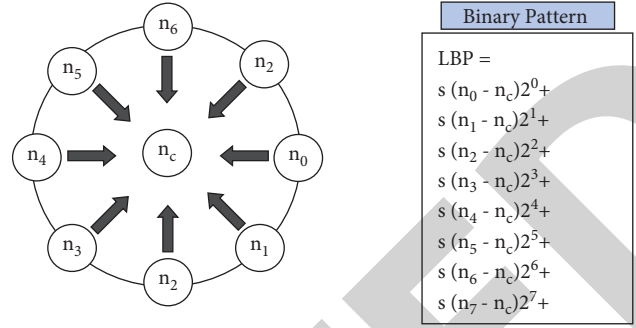


FIGURE 8: Local binary pattern.

8	4	6			
5	10	2	7	6	
1	34	3	5	10	2
0	0	0	15	34	3
0		0	0	0	0
1	1	0	0		0
			1	1	0

	12				
				12	

$$0+2^0+0+2^1+1+2^2+1+2^3+0+2^4+0+2^5+0+2^6+0+2^7=12$$

FIGURE 9: The matrix allocation of pixel values.

accordingly. Figure 10(b) shows the same picture that does not have suitable lighting conditions. The second picture is now evaluated with the ResNet model, and the results show four zebras and one horse. This erroneous output might be generated as a result of a poor lighting conditions.

After applying the mentioned modifications described in the proposed architecture to the existing model, the challenging light condition image can be subjected into bilateral filtering and adaptive sampling process that can increase the atmospheric light environment in the image. The new image can be subjected to the convolution process, and the output can be recorded. The first and third outputs are almost the same with less error. This can be indicated in Figure 11.

Figure 11 clearly shows the improvement of the detection process after the modification in the deep learning network.

## 4. Performance Evaluation

In the coco, WildTrack, and CIFAR data sets, performance may be measured using several measures such as recall, precision, and F1 score, pixel accuracy, intersection over



		
a.1 Image with proper light	b.1.Image with bad light	c.1.after correction
		
a.2.object detection	b.2.object detection	c.2.object detection
zebra : 99.92891550064087 zebra : 99.82913136482239 zebra : 98.41715693473816	zebra : 99.84723329544067 horse : 94.41177248954773 zebra : 85.79044938087463 zebra : 74.2976725101471 zebra : 72.1422553062439	zebra : 99.88270401954651 zebra : 99.81141686439514 zebra : 97.57338762283325
a.3 Probability of detection	b.3 Probability of detection	c.3 Probability of detection

FIGURE 10: Testing the dataset images.

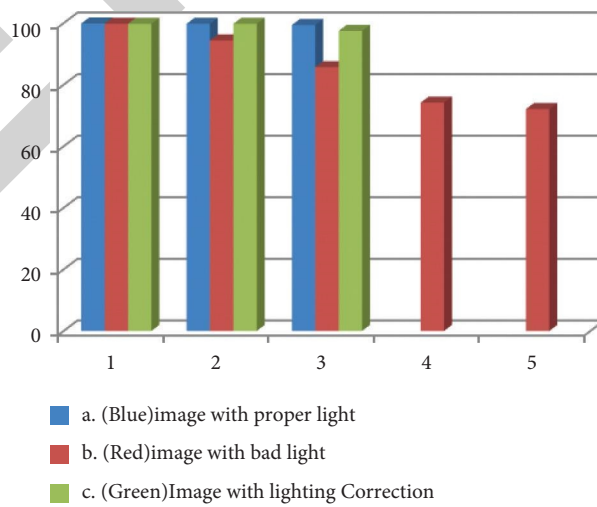


FIGURE 11: Analysis of existing and modified architecture results.

TABLE 1: Performance metrics.

Sn	Method	Precision	Recall	F1-score	Pixel accuracy	IoU	Mean IoU
1	Generative probabilistic model	64	81	75	81	80	71.3
2	ACNN model	64	91	74	90	84	79.5
3	Faster R-CNN	52	81	72	79	69	58.8
4	Gaussian mixture model	72	86	74	80	81	75.4
5	DCGAN model	66	83	72	85	79	68.9
6	Active contour mode	73	88	80	91	82	80.2
7	Dilated convolution	62	85	79	80	78	70.5
8	Edge_Constraint U-net	56	80	72	83	74	58.4
9	CSCC algorithm	67	81	76	81	77	68.4
10	Proposed model	75	84	83	90	86	84.3

union, and mean intersection over union shown in Table 1. The recall indicates how close the produced predictions are to the reality. The precision shows how the positive detections compare to the ground truth. The pixel accuracy is the proportion of pixels in a picture that are properly categorised. To give the percentage overlap between goal and projected output, the intersection over union (IoU) is also known as the Jaccard index. The average IoU metric is calculated by taking the average of all semantic class intersection over union values.

It can be concluded from the above graphs, the performance of M-ResNet can be much more improved when compared to existing methods.

## 5. Conclusion

In this work, an improved ResNet model is presented to reduce object identification faults in video surveillance systems owing to inadequate light. ResNet design uses skip connections to prevent difficulties caused by disappearing explosive gradients. Incorporating additional layers with skip connections into the current ResNet design can deliver improved results on low-light pictures in video surveillance systems without affecting performance. The new layer operations include improving illumination conditions with bilateral filtering, avoiding antialiasing effects with adaptive sampling, and improving image quality using local binary patterns. These three operations provide more precise information for further analyzing the picture in order to improve the object recognition process. This improved ResNet architecture is tested against several picture quality measures using different datasets. When compared to current approaches, the suggested method produces superior outcomes. This article has one limitation: if the processed picture has extremely low light, it takes longer to process the data for real-time photographs. Future studies will investigate ways to enhance picture illumination data in the video surveillance object recognition process without needing both low light and normal light images, which gives both higher performance and less processing time.

## Data Availability

The data that support the findings of this study are available on request to the corresponding author.

## Conflicts of Interest

The authors declare that they have no conflicts of interest to report regarding the present study.

## References

- [1] S. Ding, L. Cong, and L. Cong, "Super-pixel image segmentation algorithm based on adaptive equalisation feature parameters," *IET Image Processing*, vol. 14, no. 17, pp. 4461–4467, 2020.
- [2] Y. Wu, J. Zheng, W. Song, and F. Liu, "Low light image enhancement based on non-uniform illumination prior model," *IET Image Processing*, vol. 13, no. 13, pp. 2448–2456, 2019.
- [3] J. Zhang, Y. Wang, H. Wang, J. Wu, and Y. Li, "CNN cloud detection algorithm based on channel and spatial attention and probabilistic upsampling for remote sensing image," *IEEE Transactions on Geoscience and Remote Sensing*, vol. 60, Article ID 5404613, 2021.
- [4] D. Valsesia, G. Magli, and E. Magli, "Deep graph-convolutional image denoising," *IEEE Transactions on Image Processing*, vol. 29, pp. 8226–8237, 2020.
- [5] Q. Guo, C. Zhang, Y. Zhang, and H. Liu, "An efficient SVD-based method for image denoising," *IEEE Transactions on Circuits and Systems for Video Technology*, vol. 26, no. 5, pp. 868–880, 2015.
- [6] T. Ma, M. Guo, Z. Yu, Y. Chen, and X. Xi, R. Xincheng, Y. Li, and X. Zhou, RetinexGAN: Unsupervised low-light enhancement with two-layer convolutional decomposition networks," *IEEE Access*, vol. 9, pp. 56539–56550, 2021.
- [7] B. Li and Y. He, "An improved ResNet based on the adjustable shortcut connections," *IEEE Access*, vol. 6, pp. 18967–18974, 2018.
- [8] D. Kang, S. Park, and J. Paik, "SdBAN: salient object detection using bilateral attention network with dice coefficient loss," *IEEE Access*, vol. 8, pp. 104357–104370, 2020.
- [9] L. Sun, B. Jeon, B. N. Soomro, Y. Zheng, and Z. Wu, L. Xiao, Fast superpixel based subspace low rank learning method for hyperspectral denoising," *IEEE Access*, vol. 6, pp. 12031–12043, 2018.
- [10] W. Kim, R. Lee, M. Park, and S. H. Lee, M. S. Choi, Low-light image enhancement using volume-based subspace analysis," *IEEE Access*, vol. 8, pp. 118370–118379, 2020.
- [11] Q. Lv, W. Feng, Y. Quan, G. Dauphin, and L. Gao, M. Xing, Enhanced-random-feature-subspace-based ensemble cnn for the imbalanced hyperspectral image classification," *Ieee Journal of Selected Topics in Applied Earth Observations and Remote Sensing*, vol. 14, pp. 3988–3999, 2021.

- [12] S. Kumar, P. K. Srivastava, A. K. Pal et al., "Protecting location privacy in cloud services," *Journal of Discrete Mathematical Sciences and Cryptography*, 2022.
- [13] M. Kaur and D. Singh, "Multiobjective evolutionary optimization techniques based hyperchaotic map and their applications in image encryption," *Multidimensional Systems and Signal Processing*, vol. 32, no. 1, pp. 281–301, 2021.
- [14] C. Li, X. Qin, X. Xu, and D. Yang, G. Wei, Scalable graph convolutional networks with fast localized spectral filter for directed graphs," *IEEE Access*, vol. 8, pp. 105634–105644, 2020.
- [15] H. Su and C. Jung, "Perceptual enhancement of low light images based on two-step noise suppression," *IEEE Access*, vol. 6, pp. 7005–7018, 2018.
- [16] C. Sridhar, P. Kumar Pareek, R. Kalidoss, S. S. Jamal, P. K. Shukla, and S. J. Nuagah, "Optimal medical image size reduction model creation using recurrent neural network and GenPSOWVQ," *Journal of Healthcare Engineering*, vol. 2022, Article ID 2354866, 8 pages, 2022.
- [17] Y. Guo, Y. Lu, R. W. Liu, and M. Yang, K. T. Chui, Low-light image enhancement with regularized illumination optimization and deep noise suppression," *IEEE Access*, vol. 8, pp. 145297–145315, 2020.
- [18] Y. Xiao, A. Jiang, and J. Ye, M. W. Wang, Making of night vision: object detection under low-illumination," *IEEE Access*, vol. 8, pp. 123075–123086, 2020.
- [19] G. Chen, L. Li, W. Jin, and S. Li, "High-dynamic range, night vision, image-fusion algorithm based on a decomposition convolution neural network," *IEEE Access*, vol. 7, pp. 169762–169772, 2019.
- [20] Y. Jiang, X. Gong, D. Liu, Y. Cheng, and C. Fang, X. Shen, J. Yang, P. Zhou, and Z. Wang, Enlightengan: deep light enhancement without paired supervision," *IEEE Transactions on Image Processing*, vol. 30, pp. 2340–2349, 2021.
- [21] Y. Guo, X. Ke, and J. Zhang, "A pipeline neural network for low-light image enhancement," *IEEE Access*, vol. 7, pp. 13737–13744, 2019.
- [22] D. Xue, T. Lei, X. Jia, X. Wang, T. Chen, and A. K. Nandi, "Unsupervised change detection using multiscale and multi-resolution Gaussian-Mixture-Model guided by saliency enhancement," *Ieee Journal of Selected Topics in Applied Earth Observations and Remote Sensing*, vol. 14, pp. 1796–1809, 2020.
- [23] S. Fan, H. Yu, D. Lu, S. Jiao, and W. Xu, F. Liu, Z. Liu, CSCC: convolution split compression calculation algorithm for deep neural network," *IEEE Access*, vol. 7, pp. 71607–71615, 2019.
- [24] F. Riaz, S. Rehman, M. Ajmal, R. Hafiz, and A. Hassan, N. R. Aljohani, R. Nawaz, R. Young, M. Coimbra, Gaussian mixture model based probabilistic modeling of images for medical image segmentation," *IEEE Access*, vol. 8, pp. 16846–16856, 2020.
- [25] G. Ghimpeteanu, T. Batard, and M. Bertalmio, S. Levine, A decomposition framework for image denoising algorithms," *IEEE Transactions on Image Processing*, vol. 25, no. 1, pp. 388–399, 2016.
- [26] M. E. Helou and S. Susstrunk, "Blind universal Bayesian image denoising with Gaussian noise level learning," *IEEE Transactions on Image Processing*, vol. 29, pp. 4885–4897, 2020.
- [27] M. Luthi, T. Gerig, C. Jud, and T. Vetter, "Gaussian process morphable models," *IEEE Transactions on Pattern Analysis and Machine Intelligence*, vol. 40, no. 8, pp. 1860–1873, 2017.
- [28] O. Rippl, P. Mertens, E. König, and D. Merhof, "Gaussian anomaly detection by modeling the distribution of normal data in pretrained deep features," *IEEE Transactions on Instrumentation and Measurement*, vol. 70, pp. 1–13, 2021.
- [29] B. H. Menze, K. V. Leemput, D. Lashkari et al., "A generative probabilistic model and discriminative extensions for brain lesion segmentation—with application to tumor and stroke," *IEEE Transactions on Medical Imaging*, vol. 35, no. 4, pp. 933–946, 2015.
- [30] K. Wang and M. Z. Liu, "Object recognition at night scene based on DCGAN and faster R-CNN," *IEEE Access*, vol. 8, pp. 193168–193182, 2020.
- [31] M. Antico, F. Sasazawa, Y. Takeda, A. T. Jaiprakash, and M. L. Wille, A. K. Pandey, R. Crawford, G. Carneiro, D. Fontanarosa, Bayesian CNN for segmentation uncertainty inference on 4D ultrasound images of the femoral cartilage for guidance in robotic knee arthroscopy," *IEEE Access*, vol. 8, pp. 223961–223975, 2020.
- [32] M. Kaur, D. Singh, V. Kumar, B. B. Gupta, and A. A. Abd El-Latif, "Secure and energy efficient-based E-health care framework for green internet of things," *IEEE Transactions on Green Communications and Networking*, vol. 5, no. 3, pp. 1223–1231, 2021.
- [33] Y. Zhang, W. Zheng, K. Leng, and H. Li, "Background subtraction using an adaptive local median texture feature in illumination changes urban traffic scenes," *IEEE Access*, vol. 8, pp. 130367–130378, 2020.
- [34] E. Iqbal, A. Niaz, A. A. Memon, U. Choi, and K. N. Choi, "Saliency-driven active contour model for image segmentation," *IEEE Access*, vol. 8, pp. 208978–208991, 2020.
- [35] Z. Shao, W. Zhou, X. Deng, M. Zheng, and Q. Cheng, "Multilabel remote sensing image retrieval based on fully convolutional network," *Ieee Journal of Selected Topics in Applied Earth Observations and Remote Sensing*, vol. 13, pp. 318–328, 2020.
- [36] P. K. Pareek, C. Sridhar, R. Kalidoss et al., "IntOPMICM: intelligent medical image size reduction model," *Journal of Healthcare Engineering*, vol. 2022, Article ID 5171016, 11 pages, 2022.
- [37] S. Grosche, M. Koller, J. Seiler, and A. Kaup, "Dynamic image sampling using a novel variance based probability mass function," *IEEE Transactions on Computational Imaging*, vol. 6, pp. 1440–1450, 2020.
- [38] J. Li, Z. M. Pan, Z. H. Zhang, and H. Zhang, "Dynamic ARMA-based background subtraction for moving objects detection," *IEEE Access*, vol. 7, pp. 128659–128668, 2019.
- [39] Y. Xu, Y. Feng, Z. Xie, M. Xie, and W. Luo, "Action recognition using high temporal resolution 3D neural network based on dilated convolution," *IEEE Access*, vol. 8, pp. 165365–165372, 2020.
- [40] P. Xiang, J. Song, H. Qin, W. Tan, H. Li, and H. Zhou, "Visual attention and background subtraction with adaptive weight for hyperspectral anomaly detection," *Ieee Journal of Selected Topics in Applied Earth Observations and Remote Sensing*, vol. 14, pp. 2270–2283, 2021.
- [41] T. Yu, J. Yang, and W. Lu, "Dynamic background subtraction using histograms based on fuzzy c-means clustering and fuzzy nearness degree," *IEEE Access*, vol. 7, pp. 14671–14679, 2019.
- [42] M. Xu, P. Fu, B. Liu, and J. Li, "Multi-stream attention-aware graph convolution network for video salient object detection," *IEEE Transactions on Image Processing*, vol. 30, pp. 4183–4197, 2021.
- [43] Z. Bi, T. Zhang, P. Zhou, and Y. Li, "Knowledge transfer for out-of-knowledge-base entities: improving graph-neural-network-based embedding using convolutional layers," *IEEE Access*, vol. 8, pp. 159039–159049, 2020.

- [44] H. Xia and X. Gao, "Multi-scale mixed dense graph convolution network for skeleton-based action recognition," *IEEE Access*, vol. 9, pp. 36475–36484, 2021.
- [45] O. Oktay, E. Ferrante, K. Kamnitsas et al., T. Dawes, D. P. O'Regan, and B. Kainz, "Anatomically constrained neural networks (ACNNs): application to cardiac image enhancement and segmentation," *IEEE Transactions on Medical Imaging*, vol. 37, no. 2, pp. 384–395, 2017.
- [46] Y. Lin, X. Sun, Z. Xie, J. Yi, and Y. Zhong, "Semantic segmentation with oblique convolution for object detection," *IEEE Access*, vol. 8, pp. 25326–25334, 2020.
- [47] L. Han, X. Li, and Y. Dong, "Convolutional edge constraint-based U-net for salient object detection," *IEEE Access*, vol. 7, pp. 48890–48900, 2019.
- [48] C. Cao, B. Wang, W. Zhang et al., "An improved faster R-CNN for small object detection," *IEEE Access*, vol. 7, pp. 106838–106846, 2019.
- [49] S. Mishra, P. K. Shukla, and R. Agarwal, "Location wise opinion mining of real time twitter data using Hadoop to reduce cyber crimes," in *Proceedings of the 2nd International Conference on Data, Engineering and Applications (IDEA)*, pp. 1–6, Bhopal, India, February 2020.
- [50] R. Agarwal, P. K. Shukla, and S. Goyal, "A practical approach of network simulation," in *Detecting and Mitigating Robotic Cyber Security Risks*, pp. 12–27, University Institute of Technology RGPV, Bhopal, Madhya Pradesh, 2017.
- [51] M. Gupta, K. K. Gupta, and P. K. Shukla, "Session key based fast, secure and lightweight image encryption algorithm," *Multimedia Tools and Applications*, vol. 80, no. 7, pp. 10391–10416, 2021.
- [52] A. Ali Alnuaim, M. Zakariah, C. Shashidhar et al., "Speaker gender recognition based on deep neural networks and ResNet50," *Wireless Communications and Mobile Computing*, vol. 2022, Article ID 4444388, 13 pages, 2022.
- [53] S. Kumar, K. Kumar Dubey, A. Kumar Gautam, S. Verma, V. Kumar, and U. Mamodiya, "Detection of recurring vulnerabilities in computing services," *Journal of Discrete Mathematical Sciences and Cryptography*, 2022.
- [54] P. Deliwala, R. H. Jhaveri, and S. Ramani, "Machine learning in sdn networks for secure industrial cyber physical systems: a case of detecting link flooding attack," *International Journal of Engineering Systems Modelling and Simulation*, vol. 13, no. 1, pp. 76–84, 2022.
- [55] S. Tree Health, R. Jhaveri, P. Shukla et al., *Assessment (THA) model using advanced computer vision techniques and machine learning Inventors*, Australia Innovation Patent, Phillip, Australia, 2021.
- [56] S. S. Kushwaha, S. Joshi, D. Singh, M. Kaur, and H.-N. Lee, "Systematic review of security vulnerabilities in ethereum blockchain smart contract," *IEEE Access*, vol. 10, pp. 6605–6621, 2022.